Inorganic Chemistry

Article

pubs.acs.org/IC

A New Family of Lanthanide Borate Halides with Unusual Coordination and a New Neodymium-Containing Cationic Framework

Matthew J. Polinski,[†] Evgeny V. Alekseev,[‡,§] Victoria R. Darling,[⊥] Justin N. Cross,[†] Wulf Depmeier,[¶] and Thomas E. Albrecht-Schmitt*[,∥]

[∥]Department of Chemistry and Biochemistry, Florida State University, 95 Chieftan Way, Tallahassee, Florida 32306-4390, United States

[†]Department of Chemistry and Biochemistry, University of Notre Dame, Notre Dame, Indiana 46556, United States

[‡]Forschungszentrum Jülich GmbH, Institute for Energy and Climate Research (IEK-6), 52428 Jülich, Germany

[§]Institut für Kristallographie, RWTH Aachen University, D-52066 Aachen, Germany.

[⊥]Department of Chemistry and Physics, Saint Mary's College, Notre Dame, Indiana 46556, United States

[¶]Institut für Geowissenschaften, Universität zu Kiel, 24118 Kiel, Germany

Supporting Information

ABSTRACT: The reactions of $Ln_2O_3/CeO_2/Pr_6O_{11}$ (Ln = La–Nd, Sm), molten boric acid, and concentrated HBr or HI result in the formation of $La[B_7O_{10}(OH)_3(H_2O)Br]$, $Ln[B_6O_9(OH)_2(H_2O)_2Br]\cdot 0.5H_2O$ (Ln = Ce, Pr), $Nd_2[B_{12}O_{17.5}(OH)_5(H_2O)_4Br_{1.5}]Br_{0.5}\cdot H_2O$ (**NdBOBr**), $Sm_4[B_{18}O_{25}(OH)_{13}Br_3]$, and $Ln[B_7O_{11}(OH)(H_2O)_3I]$ (Ln = La–Nd, Sm). The lanthanide(III) centers in these compounds are found with 9-coordinate hula hoop or 10-coordinate capped triangular cupola geometries, where there are six approximately coplanar oxygen donors provided by the polyborate sheet. The sheets are formed into three-dimensional frameworks via BO_3 triangles that are roughly perpendicular to the layers. Additionally, a new cationic framework, **NdBOBr**, has been isolated. **NdBOBr** is unusual in that not only is it a cationic framework, but it is also the first trivalent f-element borate to have terminal halides bound exclusively to the base site of the hula hoop. The $Ln[B_7O_{11}(OH)(H_2O)_3I]$ (Ln = La–Nd, Sm) structures require two corner-shared BO_3 units in order to tether the layers together because of the large size of the capping iodine atom.

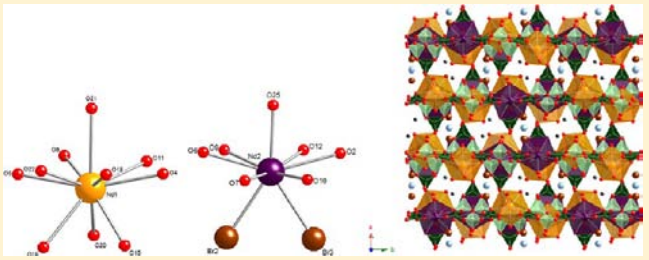

INTRODUCTION

Borates form some of the most structurally diverse polymeric networks because both BO_3 triangles and BO_4 tetrahedra can polymerize in a vast number of ways via corner- and/or edge-sharing oxygen atoms to form clusters, chains, sheets, or frameworks.[1−3] Coupled with the fact that lanthanides and actinides can adopt various geometries owing to their wide range of coordination numbers (i.e., 6–16, although seven-, eight-, and nine-coordinate are most typical),[4] f-element borates can be prepared with remarkable complexity. The intricacy of these networks can change as a function of numerous experimental conditions such as pH, temperature, stoichiometry, and reaction duration.

Historically, borates have been the subject of interest for their extraordinary optical properties.[5−8] Borates are generally transparent into the deep UV and, as such, make excellent host materials for luminescent and nonlinear-optical applications.[9] Our interest in borates, however, stems from the potential formation of actinide borates in the United States' only deep geological repository for nuclear defense waste known as the Waste Isolation Pilot Plant (WIPP).[10,11] Under repository conditions, the predominant form of the later actinides (i.e., Pu–Cm) is the trivalent (and to a lesser extent tetravalent) state, while the lanthanides, which are fission products of the actinides, will favor the trivalent state.[11] These expected oxidation states are due to the rather reducing conditions almost certain to be exhibited by the repository.[11]

WIPP is located near Carlsbad, NM, in a salt deposit known as the Salado Salt formation. This salt deposit contains several cationic and anionic species dissolved in the salt brines. Borate [mainly in the form of H_3BO_3, $B(OH)_4^-$, and $B_4O_7^{2-}$], sulfate, carbonate, and chloride are the predominate anionic species, while sodium, magnesium, and potassium are the main cationic species.[11] Additionally, calcium and bromide are also present but to a lesser degree.[11] It has been demonstrated that borate, not carbonate, is the primary complexent of trivalent metal ions under the conditions present at WIPP.[12] The presence of decaying nuclear waste will lead to heating beyond ambient conditions in the deposit, and therefore the reactions of f elements with borates at moderate temperatures are important to study in order to predict their fate in WIPP.

Received: October 19, 2012
Published: January 29, 2013

dx.doi.org/10.1021/ic302309z | Inorg. Chem. 2013, 52, 1965–1975

Table 1. Crystallographic Data for $La[B_7O_{10}(OH)_3(H_2O)Br]$ (LaBOBr), $Ce[B_6O_9(OH)_2(H_2O)_2Br]\cdot 0.5H_2O$ (CeBOBr), $Pr[B_6O_9(OH)_2(H_2O)_2Br]\cdot 0.5H_2O$ (PrBOBr), $Nd_2[B_{12}O_{17.5}(OH)_5(H_2O)_4Br_{1.5}]Br_{0.5}\cdot H_2O$ (NdBOBr), and $Sm_4[B_{18}O_{25}(OH)_{13}Br_3]$ (SmBOBr)

	LaBOBr	CeBOBr	PrBOBr	NdBOBr	SmBOBr
mass	518.49	500.89	501.68	1018.02	1643.71
color and habit	colorless, plate	colorless, plate	green, plate	purple, plate	colorless, acicular
space group	$P2_1/n$	$P2_1/n$	$P2_1/n$	$Fdd2$	$P2/c$
a (Å)	7.9440(17)	8.1507(13)	8.1346(12)	30.6651(7)	10.508(7)
b (Å)	15.105(3)	14.874(2)	14.819(2)	19.7956(4)	6.427(4)
c (Å)	9.836(2)	9.8671(15)	9.8465(15)	16.0737(5)	23.408(14)
α (deg)	90	90	90	90	90
β (deg)	90.000(3)	90.085(2)	90.153(2)	90	97.585(7)
γ (deg)	90	90	90	90	90
V (Å^3)	1180.3(4)	1196.3(3)	1187.0(3)	9757.3(4)	1566.9(17)
Z	4	4	4	16	2
T (K)	100(2)	100(2)	100(2)	100(2)	100(2)
λ (Å)	0.71073	0.71073	0.71073	0.71073	0.71073
max 2θ (deg)	27.52	27.58	27.57	27.58	27.72
ρ_{calcd} (g cm^{-3})	2.918	2.781	2.807	2.772	3.484
μ(Mo Kα)	70.84	72.15	75.41	76.04	113.54
$R(F)$ for $F_o^2 > 2\sigma(F_o^2)^a$	0.0353	0.0333	0.0262	0.0478	0.0319
$R_w(F_o^2)^b$	0.0773	0.0807	0.0567	0.1205	0.0630

$^aR(F) = \sum||F_o| - |F_c||/\sum|F_o|$. $^bR(F_o^2) = [\sum w(F_o^2 - F_c^2)^2/\sum w(F_o^4)]^{1/2}$.

Table 2. Crystallographic Data for $La[B_7O_{11}(OH)(H_2O)_3I]$ (LaBOI), $Ce[B_7O_{11}(OH)(H_2O)_3I]$ (CeBOI), $Pr[B_7O_{11}(OH)(H_2O)_3I]$ (PrBOI), $Nd[B_7O_{11}(OH)(H_2O)_3I]$ (NdBOI), and $Sm[B_7O_{11}(OH)(H_2O)_3I]$ (SmBOI)

	LaBOI	CeBOI	PrBOI	NdBOI	SmBOI
mass	581.48	582.69	583.48	586.81	592.92
color and habit	colorless, acicular	colorless, acicular	light green, acicular	purple, acicular	colorless, acicular
space group	$P2_1/n$	$P2_1/n$	$P2_1/n$	$P2_1/n$	$P2_1/n$
a (Å)	8.178(2)	8.1641(16)	8.1504(16)	8.1464(11)	8.102(4)
b (Å)	17.251(5)	17.205(4)	17.205(4)	17.199(2)	17.158(7)
c (Å)	9.849(3)	9.816(2)	9.814(2)	9.7935(13)	9.733(4)
α (deg)	90	90	90	90	90
β (deg)	90.000(4)	90.000(6)	90.0000(9)	90.0000(7)	90.000(4)
γ (deg)	90	90	90	90	90
V (Å^3)	1389.4(7)	1378.8(5)	1376.2(5)	1372.2(3)	1352.9(10)
Z	4	4	4	4	4
T (K)	100(2)	100(2)	100(2)	100(2)	100(2)
λ (Å)	0.71073	0.71073	0.71073	0.71073	0.71073
max 2θ (deg)	27.68	28.44	28.48	27.58	27.53
ρ_{calcd} (g cm^{-3})	2.780	2.807	2.816	2.841	2.911
μ(Mo Kα)	53.73	56.17	58.61	61.11	67.01
$R(F)$ for $F_o^2 > 2\sigma(F_o^2)^a$	0.0547	0.0472	0.0466	0.0517	0.0353
$R_w(F_o^2)^b$	0.1427	0.0963	0.0933	0.1289	0.0827

$^aR(F) = \sum||F_o| - |F_c||/\sum|F_o|$. $^bR(F_o^2) = [\sum w(F_o^2 - F_c^2)^2/\sum w(F_o^4)]^{1/2}$.

Because of the large cross section and neutron-capture abilities of boron, boric acid is generally used in nuclear reactors to absorb neutrons and as a corrosion inhibitor.[13] This was certainly the case during the earthquake and subsequent tsunami that crippled the Fukushima Daiichi nuclear power plant. In an effort to prevent the nuclear fuel rods from melting down, large amounts of seawater and boric acid were pumped into the reactors.[14] It is believed that the cladding of the fuel rods failed, thus exposing the hot fuel to concentrated boric acid. This event most likely produced actinide borates. Because seawater contains many dissolved ions (i.e., chloride, sodium, etc.), it is possible that these ions may have become incorporated into the resulting actinide borates.

We have recently reported on the structures of lanthanide(III) and actinide(III) borates obtained when starting with the trichloride (La–Nd, Sm–Lu; Pu–Cm),[15−17] tribromide (La–Nd; Pu),[18] and oxyiodide (La–Nd; Pu).[18] In this work, we report on the structures obtained when the lanthanide oxides, boric acid, making use of boric acid as a reactive flux media, and excess bromide and iodide obtained from concentrated HX (X = Br, I) are allowed to react.

EXPERIMENTAL SECTION

Syntheses. $La[B_7O_{10}(OH)_3(H_2O)Br]$ (LaBOBr)/$Ln[B_6O_9(OH)_2(H_2O)_2Br]\cdot 0.5H_2O$/$Nd_2[B_{12}O_{17.5}(OH)_5(H_2O)_4Br_{1.5}]0.5Br\cdot H_2O$/$Sm_4[B_{18}O_{25}(OH)_{13}Br_3]$ (SmBOBr)/$Ln[B_7O_{11}(OH)(H_2O)_3I]$. All reactants were of reagent-grade and were used as received without any further purification: Ln_2O_3 (Ln = La, Nd, Sm; Alfa Aesar, 99.99%), CeO_2 (Alfa Aesar, 99.5%), Pr_6O_{11} (Alfa Aesar, 99.9%), H_3BO_3 (Alfa Aesar, 99.5% min, ACS), HBr (Alfa Aesar, 48% w/w, 99.99%), and HI (Sigma Aldrich, 57% w/w, unstabilized, 99.99%). A total of 200 mg of a

dx.doi.org/10.1021/ic302309z | Inorg. Chem. 2013, 52, 1965−1975

lanthanide starting source (Ln_2O_3 or CeO_2 or Pr_6O_{11}) was charged into its own individual poly(tetrafluoroethylene)-lined Parr 4749 autoclave with a 23 mL internal volume and dissolved using 300 μL of either concentrated HBr (8.9 M) or HI (7.8 M). Boric acid (15:1 and 30:1 molar ratios in favor of boric acid) was then added to the sample. The samples were sealed and heated in four different ways: 200 °C for 5 days, 200 °C for 7 days, 240 °C for 5 days, and 240 °C for 7 days all under autogenous pressure, which was followed by slow cooling over a 2−3 day period. Regardless of the heating scheme, no change in product was observed. The resulting products, of which the bulk were of the appropriate color for each lanthanide (i.e., green for praesodymium, purple for neodymium, etc.), were washed extensively with boiling deionized water to remove excess boric acid. Washing was always necessary because the products were contained in a solid mass of recrystallized, colorless, and glassy-looking boric acid, and as such, these reactions did not result in pure phases. Even with repeated washings, it was difficult to completly remove all remenant borate flux. It should be noted that all products are both air- and water-stable and repeated washings did not dissolve any of the lanthanide borate products. However, after a period of approximately 6 months, the lanthanide borate iodide products began to lose their crystallinity. This is not entirely surprising given the bond length and strength of the lanthanide−iodine bond. This has been observed before in our plutonium borate iodide, which began to lose crystallinity after only a few weeks almost certainly accelerated by radiation damage.[18] After washings, the samples were plated onto Petri dishes using either methanol or ethanol and allowed to dry in air, which always resulted in some recrystallized boric acid along with the crystalline product. Approximate yields of 60−85% were observed for all products.

Crystallographic Studies. Crystals of all compounds were mounted on CryoLoops with Krytox oil and optically aligned on a Bruker APEXII Quazar X-ray diffractometer using a digital camera. Initial intensity measurements were performed using an IμS X-ray source and a 30 W microfocused sealed tube (Mo Kα, λ = 0.71073 Å) with high-brilliance and high-performance focusing Quazar multilayer optics. Standard *APEXII* software was used for determination of the unit cells and data collection control. The intensities of the reflections of a sphere were collected by a combination of four sets of exposures (frames). Each set had a different φ angle for the crystal, and each exposure covered a range of 0.5° in ω. A total of 1464 frames were collected with an exposure time per frame of 10−50 s, depending on the crystal. *SAINT* software was used for data integration including Lorentz and polarization corrections. Semi-empirical absorption corrections were applied using the program *SCALE* (*SADABS*).[19,20] Selected crystallographic information is listed in Tables 1 and 2. Atomic coordinates and additional structural information are provided in the Supporting Information (CIF).

Powder diffraction was collected on a Bruker D8 Advance with DaVinci (Cu Kα, λ = 1.5405 Å) using $\theta/2\theta$ geometry. The rotating sample was scanned from 2θ = 5° to 90° at a 0.02 step and 10 s/step. Powder patterns for the bromide species presented within were compared to calculated versions and can be found in the Supporting Information (Figures SI1−SI5). Not all samples appear to be phase-pure. Mismatched peaks correspond to boric acid. It should be noted that the iodide species presented are air-sensitive and seem to decompose over time.

RESULTS AND DISCUSSION

When reacted with boric acid and HBr (8.9 M), $Ln_2O_3/CeO_2/Pr_6O_{11}$ (Ln = La, Nd, Sm) results in the formation of four different products: $La[B_7O_{10}(OH)_3(H_2O)Br]$ (**LaBOBr**), $Ln[B_6O_9(OH)_2(H_2O)_2Br]\cdot 0.5H_2O$ (Ln = Ce, Pr), $Nd_2[B_{12}O_{17.5}(OH)_5(H_2O)_4Br_{1.5}]0.5Br\cdot H_2O$, and $Sm_4[B_{18}O_{25}(OH)_{13}Br_3]$ (**SmBOBr**).

Structures and Topological Descriptions. ***LaBOBr.*** **LaBOBr** crystallizes in the centrosymmetric, monoclinic space group $P2_1/n$ and possesses pseudoorthorhombic symmetry (Table 1). It is a dense, three-dimensional network (Figure 1a) that can be projected into the *ab* plane and is composed of only corner-sharing BO_3 triangles and BO_4 tetrahedra. Within the three-dimensional framework, and extending into the *ac* plane, are sheets (Figure 1b) made up of BO_3 and BO_4 units that create triangular holes in which the lanthanum metal centers can reside.

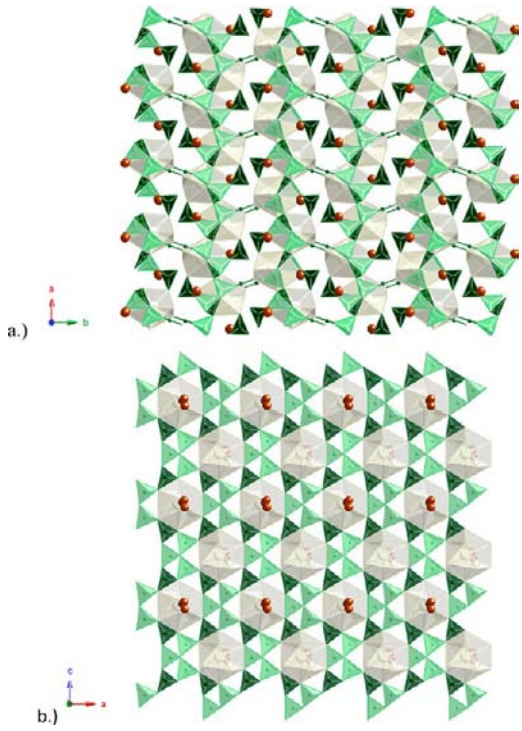

Figure 1. Depiction of the (a) three-dimensional framework and (b) sheet topology of **LaBOBr**. The lanthanum metal centers are depicted by the light-pink polyhedra, the bromine is depicted by the brown spheres, BO_4 tetrahedra are light-green units, and BO_3 triangles are dark-green units.

These triangular holes are made up of nine borate units (five BO_4 tetrahedra and four BO_3 triangles) of which two BO_3 triangles and one BO_4 tetrahedron share edges with the lanthanum coordination polyhedron. The sheets are tethered together to create the overall three-dimensional structure by a corner-shared BO_3 triangle bound to the base of the lanthanum center and connected to the borate trimer containing a μ_3 oxo unit that can be seen in the sheet topology (Figure 1b).

The polyborate sheet provides six oxygen donors that are nearly coplanar and coordinate to the metal center in the equatorial plane (Figure 2a). This mode of coordination allows for additional connections to the top (apical) and bottom (base) of the metal centers. For the lanthanum center in **LaBOBr**, the apical site is coordinated by a terminal, disordered bromide anion, while the base sites are comprised of oxygen atoms from a water moiety (O1) and two different BO_3 triangles (O2 and O5). One BO_3 unit tethers the layers together, while the other coordinates with an adjacent lanthanum center within the same sheet. This 10-coordinate geometry is best described as a capped triangular cupola[21] (Figure 2a) and, while fairly common for trivalent lanthanide and actinides in a borate matrix,[15−18,22,23] is typically not found in other lanthanide and actinide systems.[4]

The average La−Br bond length is 3.01(2) Å, and the equatorial oxygen bond lengths range from 2.575(2) to 2.727(5) Å (Table 3). The base oxygen bond lengths are 2.554(5) Å for the water moiety (O1) and 2.533(6) and 2.688(5) Å for the layer/sheet-tethering BO_3 units (O2 and O5; Table 3).

Ln[B$_6$O$_9$(OH)$_2$(H$_2$O)$_2$Br]·0.5H$_2$O. $Ln[B_6O_9(OH)_2(H_2O)_2Br]\cdot 0.5H_2O$ (Ln = Ce, Pr; **CeBOBr** and **PrBOBr**) crystallize in the centrosymmetric, monoclinic space group $P2_1/n$ (Table 1). **CeBOBr** and **PrBOBr** both form dense, three-dimensional networks (Figure 3a), which can be projected into the *ab* plane and are comprised of only corner-shared BO_3 triangles and BO_4

dx.doi.org/10.1021/ic302309z | *Inorg. Chem.* 2013, 52, 1965−1975

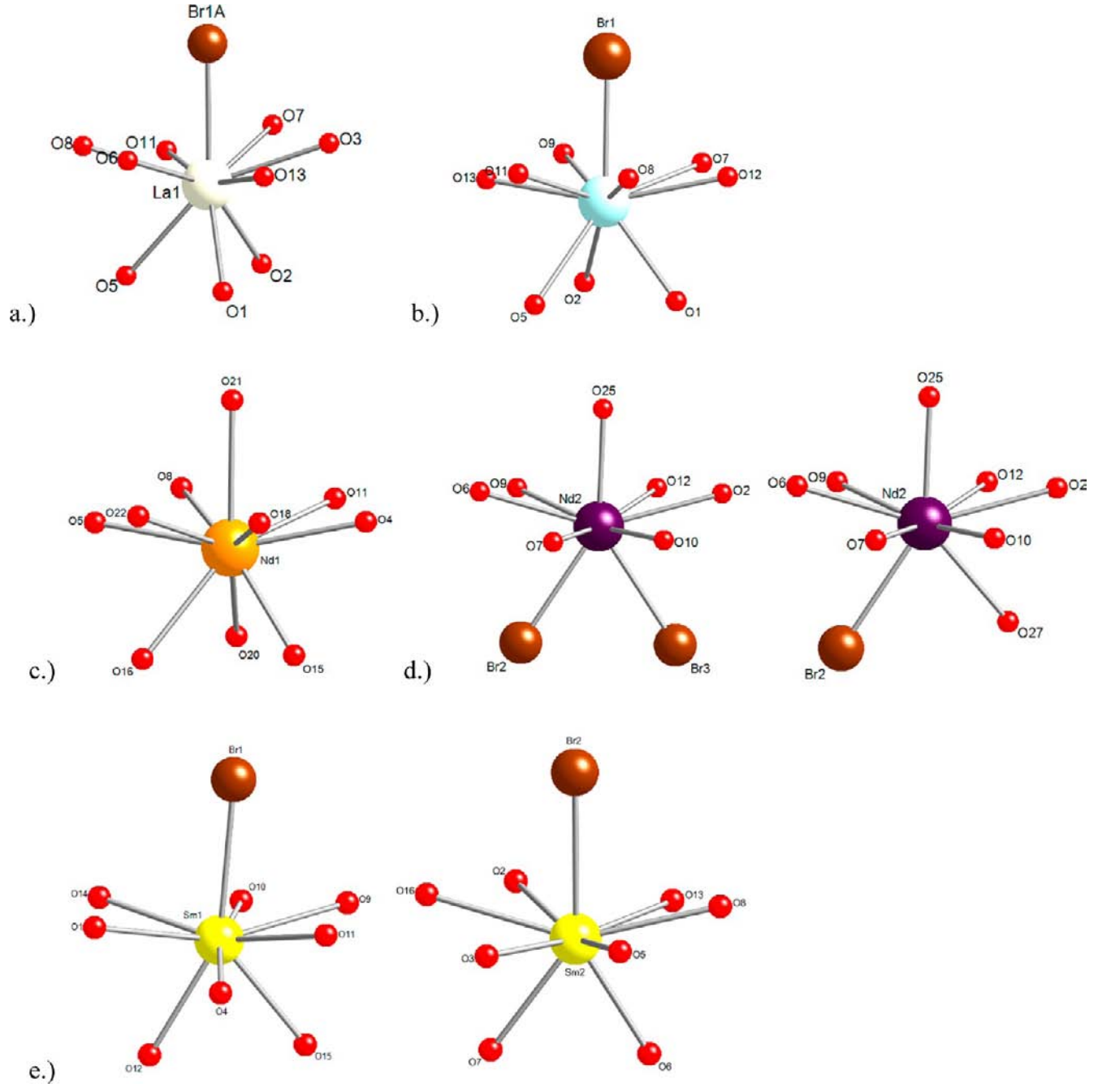

Figure 2. Coordination geometries for the lanthanide metal centers where red spheres denote oxygen atoms, brown spheres denote bromide atoms, and the remaining colored spheres are the lanthanide metal centers: (a) capped triangular cupola depicting coordination of **LaBOBr**; (b) capped triangular cupola depicting coordination of $Ln[B_6O_9(OH)_2(H_2O)_2Br]\cdot 0.5H_2O$ (Ln = Ce, Pr); (c) capped triangular cupola depicting coordination of Nd1 in **NdBOBr**; (d) hula hoop depicting coordination of Nd2 in **NdBOBr**; (e) hula hoop depicting coordination of **SmBOBr**.

tetrahedra. Within the three-dimensional framework and extending into the *ac* plane are sheets, identical with that of **LaBOBr** (Figure 1b), that are made up of nine borate units (five BO_4 tetrahedra and four BO_3 triangles) of which two BO_3 triangles and one BO_4 tetrahedron share common edges with the metal coordination polyhedron. The sheets are tethered together to create the overall three-dimensional structure by corner-shared BO_3 triangles connected to the borate trimer containing a μ_3 oxo unit that can be seen in the sheet topology (Figure 3b).

The metal centers of **CeBOBr** and **PrBOBr** are 10-coordinate with a capped triangular cupola geometry (Figure 2b).[21] This geometry is a result of the factors discussed above. The apical site is coordinated by a terminal bromide, while the base sites are now comprised of oxygen atoms from two water moieties (O1 and O2) and one layer-tethering BO_3 triangle (O5; Figure 3b). While the apical bromides are terminal, they do point toward one another with an approximate 5.2 Å separation (Figure 3a). This creates rather large hourglass/bowtie-shaped holes in the three-dimensional framework in which the half-occupied, unbound water molecules reside (Figure 3b). This void space in the three-dimensional framework also allows room for the water molecules bound to the base sites of the metal centers to reside.

For **CeBOBr** and **PrBOBr**, the equatorial oxygen bond lengths range from 2.579(3) to 2.733(4) Å and from 2.565(3) to

dx.doi.org/10.1021/ic302309z | *Inorg. Chem.* 2013, 52, 1965−1975

Table 3. Selected Bond Distances (Å) for LaBOBr, CeBOBr, and PrBOBr

distance (Å)							
equatorial		base		equatorial		base	
La1−Br1[a]	3.01(2)	La1−O1	2.554(5)	Pr1−Br1	2.9537(7)	Pr1−O1	2.515(3)
La1−O3	2.724(5)	La1−O2	2.533(6)	Pr1−O7	2.663(3)	Pr1−O2	2.409(3)
La1−O6	2.711(5)	La1−O5	2.688(5)	Pr1−O8	2.651(3)	Pr1−O5	2.683(3)
La1−O7	2.727(5)			Pr1−O9	2.728(3)		
La1−O8	2.713(5)			Pr1−O11	2.612(3)		
La1−O11	2.572(5)			Pr1−O12	2.595(3)		
La1−O13	2.609(5)			Pr1−O13	2.565(3)		
Ce1−Br1	2.9758(8)	Ce1−O1	2.526(5)				
Ce1−O7	2.679(3)	Ce1−O2	2.428(5)				
Ce1−O8	2.671(3)	Ce1−O5	2.692(4)				
Ce1−O9	2.733(4)						
Ce1−O11	2.624(3)						
Ce1−O12	2.608(3)						
Ce1−O13	2.579(3)						

[a]Average bond length of disordered bromide anions.

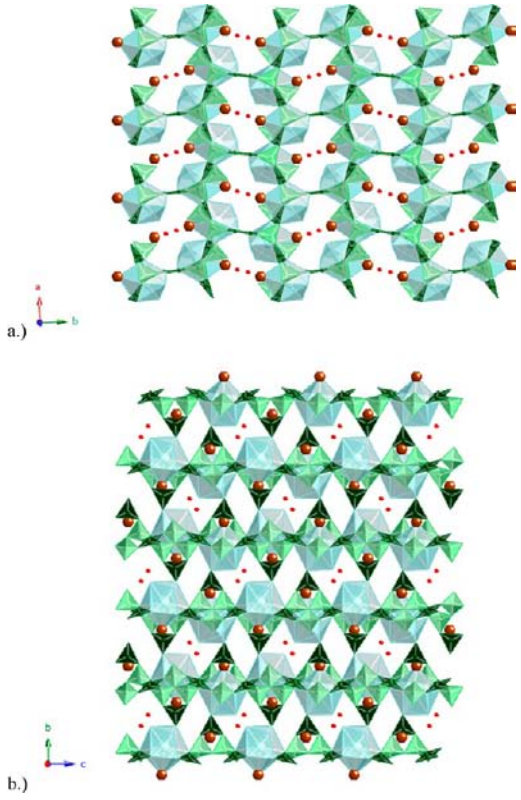

Figure 3. Depiction of the three-dimensional framework of Ln-$[B_6O_9(OH)_2(H_2O)_2Br]\cdot 0.5H_2O$ (Ln = Ce, Pr) viewed down the (a) *c* and (b) *a* axes. The lanthanide metal centers are depicted by light-blue polyhedra, the bromine atoms are depicted by brown spheres, BO_4 tetrahedra are light-green units, BO_3 triangles are dark-green units, and the cocrystallized water molecules are red spheres.

2.728(3) Å, respectively. The base water (O1 and O2) bond lengths are 2.526(5) and 2.428(5) Å and 2.515(3) and 2.409(3) Å with the oxygen atom of the BO_3 unit (O5) at 2.692(4) and 2.683(3) Å for **CeBOBr** and **PrBOBr**, respectively. Finally, the Ln−Br bond lengths are 2.9758(8) and 2.9537(7) Å for **CeBOBr** and **PrBOBr**, respectively (Table 3).

NdBOBr. **NdBOBr** crystallizes in the polar, orthorhombic space group *Fdd*2. It is a unique lanthanide borate for several reasons but most noticeably in that it forms a three-dimensional cationic framework (Figure 4a). **NdBOBr** contains two independent neodymium metal centers with differing coordination numbers and ligands. The first neodymium center (Nd1) is 10-coordinate with a capped triangular cupola geometry (Figure 2c).[21] This geometry is achieved by the six nearly coplanar oxygen atoms donated by two edge-sharing BO_3 units and one edge-sharing BO_4 unit found within the sheet topology (Figure 4b), an apical water moiety (O21), two base water moieties (O15 and O20), and one layer-tethering BO_3 unit (O16) on the third base site. This layer-tethering BO_3 unit coordinates to the borate trimer containing a μ_3 oxo unit that can be found within the sheet (Figure 4) and is the only mode of connection between the sheets.

The second neodymium center (Nd2) is nine-coordinate with a geometry best described as a hula hoop (Figure 2d).[24] This geometry is achieved by six nearly coplanar oxygen atoms donated by two edge-sharing BO_3 units and one edge-sharing BO_4 unit found within the sheet topology (Figure 4b), an apical water moiety (O25), and either two base bromides (Br2 and Br3) or a bromide (Br2) and a hydroxide moiety (O27). It should be noted that Br3 and O27 partially occupy the same position (i.e., half-occupied).

The sheet topology is very similar to that seen in **LaBOBr**, **CeBOBr**, and **PrBOBr**; however, **NdBOBr** contains diagonal rows of Nd1 and Nd2 polyhedra (Figure 4b). The sheets are connected via the BO_3 unit on the base of the Nd1 site to the μ_3 borate oxo unit of the sheet above or below it. Furthermore, upon viewing down the *b* axis, there are two different and rather large holes in the three-dimensional framework (Figure 4a). The first is an hourglass/bowtie-shaped hole that contains the unbound water molecules as well as the hydroxide and bound water molecules to the base sites of both Nd1 and Nd2. The second is a diamond-shaped hole that contains an unbound, free bromide anion. The presence of an uncoordinated bromide anion strongly suggests that the framework is indeed a cationic framework.

For **NdBOBr**, the equatorial oxygen bond lengths range from 2.547(6) to 2.676(6) Å and from 2.494(5) to 2.651(5) Å for Nd1 and Nd2, respectively, with capping water bond distances at 2.706(8) Å (O21) and 2.453(8) Å (O25). The base water distances are 2.423(6) Å (O15) and 2.438(7) Å (O20), the hydroxide oxygen atom distance is at 2.559 Å (O27), and the oxygen atom of the BO_3 unit (O16) on Nd1 is at a length of 2.618(3) Å. The base bromide bond lengths to Nd2 are 2.9053(14) and 2.968(2) Å for Br2 and Br3, respectively (Table 4).

dx.doi.org/10.1021/ic302309z | *Inorg. Chem.* 2013, 52, 1965−1975

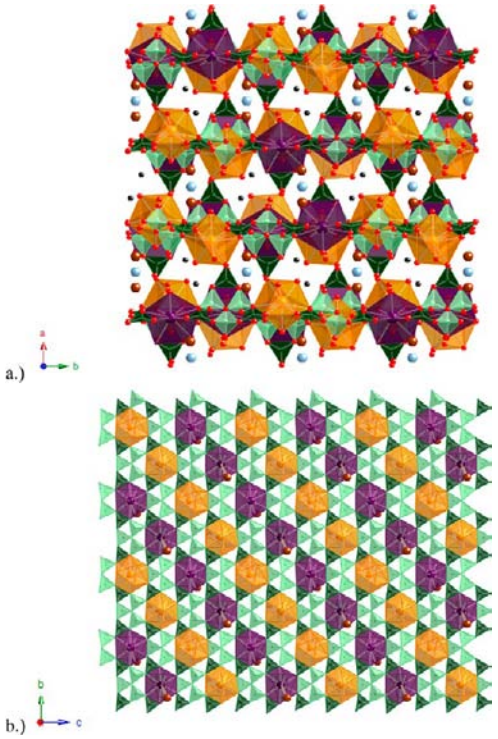

Figure 4. Depiction of the (a) three-dimensional framework and (b) sheet topology of **NdBOBr**. The neodymium metal centers are depicted by orange (Nd1) and purple (Nd2) polyhedra, the bromine atoms are depicted by brown spheres, BO_4 tetrahedra are light-green units, BO_3 triangles are dark-green units, oxygen atoms are red spheres, cocrystallized water molecules are black spheres, and unbound, free bromide anions are gray spheres.

SmBOBr. **SmBOBr** is the final compound obtained from the concentrated HBr reaction scheme. It crystallizes in the centrosymmetric, monoclinic space group $P2/c$. This compound also possesses a dense, but different, three-dimensional structure (Figure 5a) as well as a different sheet topology (Figure 5b). Like the aforementioned lanthanide bromide compounds, nine corner-sharing BO_3 and BO_4 units create triangular holes; however, in this structure, two BO_4 tetrahedra and one BO_3 triangle chelate the samarium centers. This arrangement of the polyborate network was found for some uranyl borates.[25] A projection of the three-dimensional framework into the *ac* plane can be seen in Figure 5a, while the sheet extending along the *ab* plane is shown in Figure 5b.

The samarium centers possess a capping bromide anion that is either terminal (Sm1) or bridged (Sm2) (Figure 5a). All centers are nine-coordinate with a hula-hoop geometry (Figure 2e) ascribed to the same factors presented above.[24] The additional ligands are two oxygen atoms from either an oxygen atom from a BO_3 group (O7) and a hydroxide (O6) (nonbridged center, Sm1) or two BO_4 groups (O12 and O15) (bridged center, Sm2). The layers are connected to one another by a base, corner-sharing BO_3 triangle connected to two BO_4 tetrahedra, which are coordinated to the samarium metal centers in the equatorial plane. Unlike the other bromide compounds, **SmBOBr** also has the additional tethering of layers by use of the bridging bromide (Figure 5a).

The Sm−Br bond length in the bridged **SmBOBr** center is 2.8924(16) Å, while the terminal bromide center has a Sm−Br bond length of 2.9350(15) Å. The equatorial bond lengths range from 2.443(4) to 2.581(4) Å on Sm1 (unbridged) with base oxygen lengths of 2.460(4) and 2.464(4) Å for O12 and O15 of the different BO_4 units, respectively. The equatorial bond lengths range from 2.478(4) to 2.681(4) Å on Sm2 (bridged) with base oxygen lengths of 2.362(5) and 2.458(5) Å for the hydroxide (O6) and BO_3 unit (O7), respectively (Table 4).

$Ln[B_7O_{11}(OH)(H_2O)_3I]$. When reacted with boric acid and HI (7.8 M), $Ln_2O_3/CeO_2/Pr_6O_{11}$ (Ln = La, Nd, Sm) results in the formation of one product: $Ln[B_7O_{11}(OH)(H_2O)_3I]$. $Ln[B_7O_{11}(OH)(H_2O)_3I]$ (Ln = La−Nd, Sm) crystallizes in the centrosymmetric, monoclinic space group $P2_1/n$ (Table 2) and possesses pseudoorthorhombic symmetry.

These compounds, herein referred to as **LaBOI**, **CeBOI**, **PrBOI**, **NdBOI**, and **SmBOI** for the corresponding lanthanide borate iodide, each form a dense, three-dimensional framework (Figure 6a) comprised of only corner-shared BO_3 triangles and BO_4 tetrahedra. The three-dimensional framework is comprised of sheets (Figure 1b), identical with those of **LaBOBr**, **CeBOBr**, and **PrBOBr**, which extend into the *ac* plane. Unlike the other three-dimensional frameworks presented in this work, the most noticeable difference present in the **LnBOI** structures is the use of two, end-to-end, corner-sharing BO_3 units necessary to tether the layers together. These layer-tethering BO_3 units are not bound to the metal center in any way. In fact, they are only bound

Table 4. Selected Bond Distances (Å) for NdBOBr and SmBOBr

distance (Å)							
equatorial		base		equatorial		base	
Nd1−O21	2.706(8)	Nd1−O15	2.423(6)	Sm1−Br1	2.9350(15)	Sm1−O12	2.460(4)
Nd1−O4	2.584(5)	Nd1−O16	2.618(6)	Sm1−O1	2.553(4)	Sm1−O15	2.464(4)
Nd1−O5	2.611(5)	Nd1−O20	2.438(7)	Sm1−O4	2.480(5)		
Nd1−O8	2.676(6)			Sm1−O9	2.581(4)		
Nd1−O11	2.632(5)			Sm1−O10	2.443(4)		
Nd1−O18	2.657(6)			Sm1−O11	2.513(4)		
Nd1−O22	2.547(6)			Sm1−O14	2.502(4)		
Nd2−O25	2.453(8)	Nd2−Br2	2.9053(14)	Sm2−Br2	2.8924(16)	Sm2−O6	2.362(5)
Nd2−O2	2.651(5)	Nd2−Br3	2.968(2)	Sm2−O2	2.502(4)	Sm2−O7	2.458(5)
Nd2−O6	2.584(6)	Nd2−O27	2.559(13)	Sm2−O3	2.528(5)		
Nd2−O7	2.503(6)			Sm2−O5	2.478(4)		
Nd2−O9	2.566(5)			Sm2−O8	2.530(4)		
Nd2−O10	2.502(6)			Sm2−O13	2.644(5)		
Nd2−O12	2.494(5)			Sm2−O16	2.681(4)		

dx.doi.org/10.1021/ic302309z | *Inorg. Chem.* 2013, 52, 1965−1975

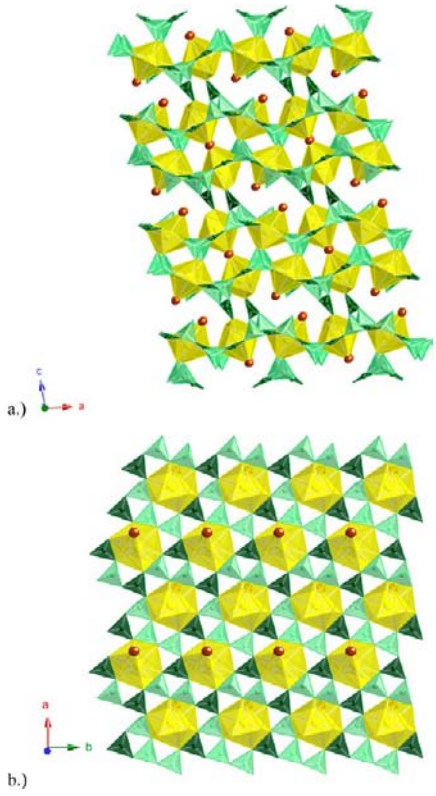

Figure 5. Depiction of the (a) three-dimensional framework and (b) sheet topology of **SmBOBr**. The samarium metal centers are depicted by yellow spheres, the bromine atoms are depicted by brown spheres, BO_4 tetrahedra are light-green units, and BO_3 triangles are dark-green units.

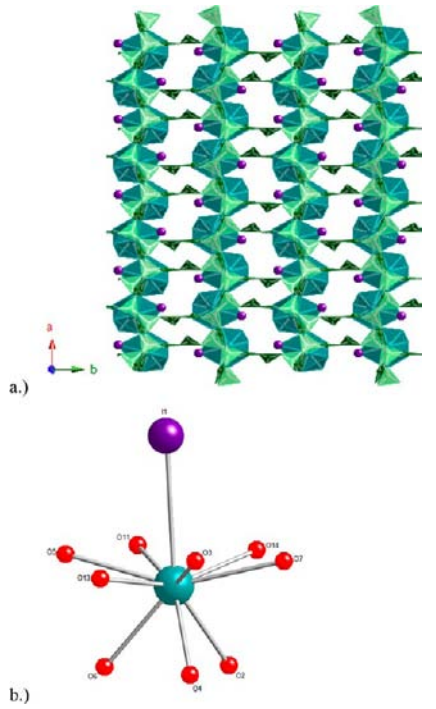

Figure 6. Depiction of the (a) three-dimensional framework and (b) capped triangular cupolar geometry of $Ln[B_7O_{11}(OH)(H_2O)_3I]$ (Ln = La–Nd, Sm). The lanthanide metal centers are depicted by turquoise spheres, iodine atoms are depicted by purple spheres, BO_4 tetrahedra are light-green units, and BO_3 triangles are dark-green units, and oxygen atoms are red spheres.

above and below the corner-sharing borate trimer containing the μ_3-oxo units within the sheet. The reason for such a unique mode of tethering is due to the large capping iodide units bound to the metal centers (Figure 6b). The iodides reside in rather large holes that are present in the framework and point toward one another with an approximate 6.5 Å separation. Also present in the holes are the three bound base water units.

The metal centers are 10-coordinate with the capped triangular cupola geometry (Figure 6b).[21] Residing in the apical position are terminal iodides and, along with three water units (O2, O4, and O6) found on the base sites, complete the variable coordination sites of the capped triangular cupola. The equatorial oxygen bond lengths range from 2.506(5) to 2.761(7) Å for **LaBOI**, **CeBOI**, **PrBOI**, **NdBOI**, and **SmBOI**, with O13 being the shortest and O3 the longest equatorial bond lengths (Table 5). The base water bond lengths range from 2.449(5) to 2.584(8) Å. Finally, the Ln–I bond lengths are 3.425(13), 3.3759(11), 3.3752(11), 3.3651(10), and 3.3498(15) Å for **LaBOI**, **CeBOI**, **PrBOI**, **NdBOI**, and **SmBOI**, respectively (Table 5). The decrease in the bond lengths, unit cell constants, and volume across this isotypic series is to be expected as the lanthanide contraction is observed.

Periodic Trends. The reactions of $Ln_2O_3/CeO_2/Pr_6O_{11}$ (Ln = La, Nd, Sm) with either concentrated HBr or HI in a boric acid flux result in individual/discrete compounds for the former and an isostructural series of compounds for the latter. The compounds presented in this work share some similarities and yet vast differences. With the exception of **SmBOBr** and to some extent **NdBOBr**, all other compounds exhibit the same sheet topology sans the identity of the halide. All reported species have either a 10-coordinate capped triangular cupola geometry (**LaBOBr**, **CeBOBr**, **PrBOBr**, **NdBOBr**, and **LnBOI**) or a 9-coordinate hula-hoop geometry (**NdBOBr** and **SmBOBr**), with **NdBOBr** containing neodymium centers exhibiting both types of geometries.

The area of greatest variability in all compounds is the identity of the base units particularly that of the oxygen-containing moieties bound to the lanthanide metal centers. These oxygen-containing moieties are either BO_3 triangles or water molecules, where the BO_3 units provide a means of tethering the layers together and the water molecules, along with the capping halide atoms, help create rather large void spaces in the three-dimensional framework. This variability in the identity of the base site units accounts for the differences in the overall three-dimensional structure observed. Furthermore, with the exception of **SmBOBr**, which contains one bridging bromide and one terminal bromide, all of the capping halides are terminal and point toward one another with an approximate separation of 5.6, 5.2, 5.2, and 6.5 Å for **LaBOBr**, **CeBOBr**, **PrBOBr**, and **LnBOI**, respectively.

One of the hallmarks of this work is the synthesis of the cationic framework structure **NdBOBr**. This compound is unique for many reasons. To begin, it is the first trivalent lanthanide or actinide borate that we have prepared that crystallizes with symmetry higher than monoclinic. Next, it is a cationic framework material, which is not only rare for f-block materials but also for materials in general; the most well-known cationic materials are the layered double hydroxides.[26] It is also the second cationic framework derived from a borate matrix. We have previously reported on $[ThB_5O_6(OH)_6]$-$[BO(OH)_2]\cdot 2.5H_2O$ (NDTB-1),[27,28] which is a supertetrahedral cationic framework that is selective in the removal of TcO_4^- from solution in the presence of other similarly sized and charged anions.

dx.doi.org/10.1021/ic302309z | Inorg. Chem. 2013, 52, 1965–1975

Table 5. Selected Bond Distances (Å) for $La[B_7O_{11}(OH)(H_2O)_3I]$ (LaBOI), $Ce[B_7O_{11}(OH)(H_2O)_3I]$ (CeBOI), $Pr[B_7O_{11}(OH)(H_2O)_3I]$ (PrBOI), $Nd[B_7O_{11}(OH)(H_2O)_3I]$ (NdBOI), and $Sm[B_7O_{11}(OH)(H_2O)_3I]$ (SmBOI)

distance (Å)							
equatorial		base		equatorial		base	
La1−I1	3.4251(13)	La1−O2	2.584(8)	Nd1−I1	3.3651(10)	Nd1−O2	2.539(8)
La1−O3	2.761(7)	La1−O4	2.559(7)	Nd1−O3	2.720(8)	Nd1−O4	2.482(9)
La1−O5	2.642(6)	La1−O6	2.568(7)	Nd1−O5	2.591(7)	Nd1−O6	2.510(8)
La1−O7	2.613(7)			Nd1−O7	2.593(7)		
La1−O11	2.645(6)			Nd1−O11	2.604(8)		
La1−O13	2.559(7)			Nd1−O13	2.533(7)		
La1−O14	2.615(7)			Nd1−O14	2.584(7)		
Ce1−I1	3.3759(11)	Ce1−O2	2.554(7)	Sm1−I1	3.3498(15)	Sm1−O2	2.502(6)
Ce1−O3	2.729(6)	Ce1−O4	2.505(7)	Sm1−O3	2.719(5)	Sm1−O4	2.449(5)
Ce1−O5	2.612(7)	Ce1−O6	2.536(7)	Sm1−O5	2.588(5)	Sm1−O6	2.468(5)
Ce1−O7	2.599(6)			Sm1−O7	2.569(5)		
Ce1−O11	2.622(6)			Sm1−O11	2.581(5)		
Ce1−O13	2.532(6)			Sm1−O13	2.506(5)		
Ce1−O14	2.586(6)			Sm1−O14	2.546(5)		
Pr1−I1	3.3752(11)	Pr1−O2	2.552(7)				
Pr1−O3	2.727(6)	Pr1−O4	2.504(7)				
Pr1−O5	2.612(6)	Pr1−O6	2.532(7)				
Pr1−O7	2.596(6)						
Pr1−O11	2.616(6)						
Pr1−O13	2.532(6)						
Pr1−O14	2.586(6)						

The anion-exchange abilities of **NdBOBr** are currently being investigated and will be reported elsewhere.

NdBOBr has an unusual arrangement about the metal centers. Prior to this work, halogens were only found to be present on the apical/capping site of the hula-hoop or capped triangular cupola geometry.[15−18,22,23] The only compound that even slightly deviates from this is $Ln[B_4O_6(OH)_2Cl]$ (Ln = La−Nd, Pu) in which each apical chloride is bridged to another metal center and coordinated to the base site of the second metal center.[17] In **NdBOBr**, the bromides are found exclusively on the base sites of Nd2 and are terminal. It should be noted that when $^{242}PuO_2$ was treated with concentrated HBr and allowed to react in a boric acid flux, a very similar compound emerged, but the crystals were of poor quality and highly disordered.

The isostructural series, $Ln[B_7O_{11}(OH)(H_2O)_3I]$ (Ln = La−Nd, Sm), is a more cohesive set compared to their borate bromide counterparts but are still unique in their own right. The **LnBOI** compounds require two "end-to-end" BO_3 units bound to the μ_3 borate oxo unit within the sheets to tether the layers together. These are the first halogenated lanthanide borates to date to contain a "double" connection between the layers and the first trivalent borate species to not use any coordinate modes of the metal to contribute to layer tethering. It is not surprising that more space is needed between the sheets because iodide is a large anion. In fact, the only other halogenated borate that we have prepared that requires a "double" connection, albeit different, is $Pu^{III}[B_7O_{11}(OH)(H_2O)_2I]$ (Figure 7).[18]

$Pu[B_7O_{11}(OH)(H_2O)_2I]$ and the **LnBOI** compounds share very similar unit cell constants (sans the pseudoorthorhombic symmetry of the latter), an identical sheet topology, and the same geometry about the metal centers. There are two major differences between these species. The first is the mode of tethering of the layers, and the second is the number of water moieties bound to the base sites of the metal centers; $Pu[B_7O_{11}(OH)(H_2O)_2I]$ contains only two base water moieties,

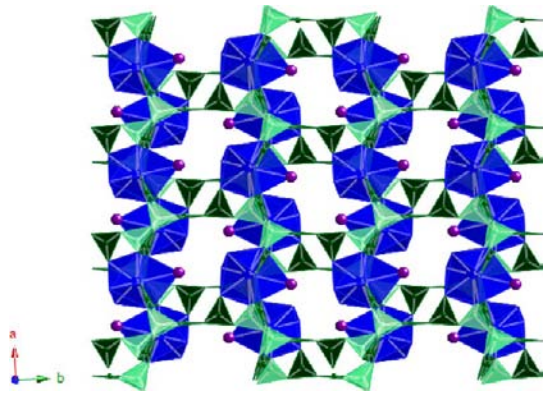

Figure 7. Depiction of the three-dimensional framework of $Pu^{III}[B_7O_{11}(OH)(H_2O)_2I]$, where the dark-blue polyhedra represent the plutonium metal centers, iodine atoms are depicted by purple spheres, BO_4 tetrahedra are light-green units, and BO_3 triangles are dark-green units.

whereas the **LnBOI** compounds contain three. Furthermore, all of the bond lengths in the **LnBOI** compounds are comparable to those seen in $Pu[B_7O_{11}(OH)(H_2O)_2I]$.[18] The **LnBOI** compounds are the only lanthanide borates that we have prepared that contain only water molecules on the base sites.

We have previously reported on the compounds obtained when the lanthanide tribromides and oxyiodides are synthesized in a boric acid flux at the same temperatures and times as those used in this work.[18] While a more complete and detailed analysis can be found elsewhere,[18] it is important to discuss some of the major features of the previous work in order to adequately compare and contrast them to their appropriate counterparts in this work (Table 6). The unbalanced reaction schemes for this study can be seen in eqs 1 (Figures 1−5) and 2 (Figure 6), while those of the previous study can be seen in eqs 3 (Figure 8) and 4 (Figure 8).

dx.doi.org/10.1021/ic302309z | Inorg. Chem. 2013, 52, 1965−1975

Table 6. Comparison of the Compounds from Current and Previous Studies with Key Structural and Geometrical Characteristics of the Central Metal Site Identified

compound	equatorial oxygen donors	identity of basal ligands	coordination number	halide coordination mode
		Current Study		
LaBOBr	2 BO_3/1 BO_4	1 H_2O/2 BO_3	10	apical, terminal
$Ln[B_6O_9(OH)_2(H_2O)_2Br]\cdot 0.5H_2O$ (Ln = Ce, Pr)	2 BO_3/1 BO_4	2 H_2O/1 BO_3	10	apical, terminal
NdBOBr	2 BO_3/1 BO_4	2 H_2O/1 BO_3 Br/OH	9 and 10	base, terminal
SmBOBr	1 BO_3/2 BO_4	1 BO_3/OH 2 BO_4	9	apical, terminal/bridging
$Ln[B_7O_{11}(OH)(H_2O)_3I]$ (Ln = La–Nd, Sm)	2 BO_3/1 BO_4	3 H_2O	10	apical, terminal
		Previous Study		
$Ln[B_5O_8(OH)(H_2O)_2Br]$ (Ln = La–Pr)	2 BO_3/1 BO_4	1 BO_3/2 H_2O	10	apical, terminal
$Nd_4[B_{18}O_{25}(OH)_{13}Br_3]$	1 BO_3/2 BO_4	1 BO_3/OH 2 BO_4	9	apical, terminal/bridging
$Ln[B_5O_8(OH)(H_2O)_2I]$ (Ln = La–Nd)	2 BO_3/1 BO_4	1 BO_3/2 H_2O	10	apical, terminal

$$Ln_2O_3 + H_3BO_3 + HBr \rightarrow La[B_7O_{10}(OH)_3(H_2O)Br] + Ln[B_6O_9(OH)_2(H_2O)_2Br]\cdot 0.5H_2O\ (Ln = Ce,\ Pr) + Nd_2[B_{12}O_{17.5}(OH)_5(H_2O)_4Br_{1.5}]Br_{0.5}\cdot H_2O + Sm_4[B_{18}O_{25}(OH)_{13}Br_3] \quad (1)$$

$$Ln_2O_3 + H_3BO_3 + HI \rightarrow Ln[B_7O_{11}(OH)(H_2O)_3I]\ (Ln = La–Nd,\ Sm) \quad (2)$$

$$LnBr_3\cdot xH_2O + H_3BO_3 \rightarrow Ln[B_5O_8(OH)(H_2O)_2Br]\ (Ln = La–Pr) + Nd_4[B_{18}O_{25}(OH)_{13}Br_3] \quad (3)$$

$$LnOI\cdot xH_2O + H_3BO_3 \rightarrow Ln[B_5O_8(OH)(H_2O)_2I]\ (Ln = La–Nd) \quad (4)$$

When $LnBr_3$ or LnOI (Ln = La–Nd, Sm) are reacted with boric acid, the following products are obtained: $Ln[B_5O_8(OH)(H_2O)_2Br]$ (Ln = La–Pr), $Ln[B_5O_8(OH)(H_2O)_2I]$ (Ln = La–Nd), and $Nd_4[B_{18}O_{25}(OH)_{13}Br_3]$.[18] It should be noted that $Ln[B_5O_8(OH)(H_2O)_2Br]$ (Ln = La–Pr) and $Ln[B_5O_8(OH)(H_2O)_2I]$ are isotypic and crystallize in the monoclinic space group $P2_1/n$ ($a \approx 6.5$ Å, $b \approx 15.3$ Å, $c \approx 10.7$ Å, and $\beta \approx 90.2°$), while $Nd_4[B_{18}O_{25}(OH)_{13}Br_3]$ is also monoclinic but crystallizes in the space group $P2/c$ and is isotypic with **SmBOBr** of this work.

The metal centers in these compounds are either 10-coordinate with a capped triangular cupola geometry ($Ln[B_5O_8(OH)(H_2O)_2Br]$ (Ln = La–Pr) and $Ln[B_5O_8(OH)(H_2O)_2I]$ (Ln = La–Nd)) or 9-coordinate with a hula-hoop geometry ($Nd_4[B_{18}O_{25}(OH)_{13}Br_3]$). These geometries are possible because of the polyborate sheet topology providing six nearly coplanar oxygen atoms from either two corner-shared BO_3 units and one corner-shared BO_4 unit in the $Ln[B_5O_8(OH)(H_2O)_2Br]$ (Ln = La–Pr) and $Ln[B_5O_8(OH)(H_2O)_2I]$ (Ln = La–Nd) species or the reverse in the $Nd_4[B_{18}O_{25}(OH)_{13}Br_3]$ compound. The halides are all terminal and reside in the apical position except for $Nd_4[B_{18}O_{25}(OH)_{13}Br_3]$, which contains both a bridging bromide and a terminal bromide residing in the apical position. Finally, the layers are tethered together exclusively by a BO_3 unit bound to a base site of the metal center to a BO_4 unit that can be seen in the sheet (Table 6). Note that the μ_3 borate oxo unit is absent even though the space group types of the previous species are identical with those of some of the new species of this work. The sheet topology and three-dimensional framework of $Ln[B_5O_8(OH)(H_2O)_2Br]$ (Ln = La–Pr) and $Ln[B_5O_8(OH)(H_2O)_2I]$ (Ln = La–Nd) can be seen in Figure 8, while those of $Nd_4[B_{18}O_{25}(OH)_{13}Br_3]$ can be seen in Figure 5 because it is isotypic with the compound **SmBOBr** of this work.

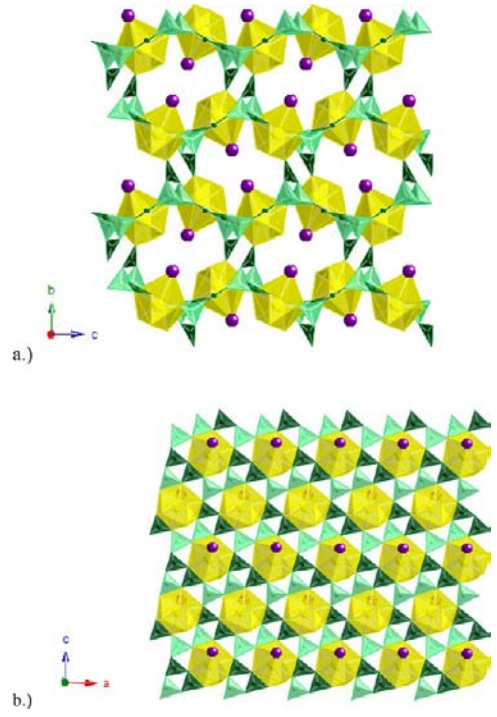

Figure 8. Depiction of the (a) three-dimensional framework and (b) sheet topology of $La[B_5O_8(OH)(H_2O)_2Br]$ (Ln = La–Pr) and $La[B_5O_8(OH)(H_2O)_2I]$ (Ln = La–Nd). The lanthanide metal centers are depicted by yellow polyhedra, the halides (Br and I) are depicted by purple spheres, BO_4 tetrahedra are light-green units, and BO_3 triangles are dark-green units. See eqs 3 and 4.

While it may appear at first glance that the former[18] and present series are very similar, there are indeed many differences, and an interesting picture emerges when they are compared (Table 6). First, lanthanum through praseodymium in the tribromide system and lanthanum through neodymium in the oxyiodide system form an isotypic set (Figure 8), while the concentrated HBr set results in individual/discrete compounds and the concentrated HI set yields a different isotypic series. Second, the neodymium compound in the tribromide set is

dx.doi.org/10.1021/ic302309z | Inorg. Chem. 2013, 52, 1965–1975

different from the other tribromide species and yet isotypic with the samarium borate bromide presented in this work. It should be noted that the compound **SmBOBr** could only be isolated by reaction with excess bromide. Next, while $Ln[B_5O_8(OH)(H_2O)_2Br]$ (Ln = La–Pr) and $Ln[B_5O_8(OH)(H_2O)_2I]$ (Ln = La–Nd) crystallize in the monoclinic system $P2_1/n$, just like the majority of the compounds in this work, the three-dimensional framework and sheet topologies are different (Figures 1, 3, and 6). The sheet topology of the tribromide/oxyiodide species is arranged in such a manner that two BO_3 units and one BO_4 unit, like that observed in **LaBOBr**, **CeBOBr**, **PrBOBr**, **NdBOBr**, and **LnBOI**, create a triangular hole in which the metal center resides. However, the difference between the sheet topologies is in the arrangement of the four BO_3 and five BO_4 units that surround the metal center (i.e., the lack of the μ_3 borate oxo unit from the tribromide/oxyiodide species). It should be noted that, generally, the metal centers in the sheet topologies of lanthanide and actinide borates are made up for nine borate units and can be derived from any combination of BO_3 and BO_4 units.[25]

To date, a total of 11 different sheet topologies have been observed for f-element borates.[25] Thus, the same geometry about the metal centers can be obtained even if the sheet topology is different. The difference in the overall structure is largely affected by the arrangement of the polyborate sheet, the layer-tethering units of the base sites, and the terminal/bridging nature of the unit in the apical position (which can be a halogen or a borate unit).[15−18,22,23,25,29]

In the previously published tribromide/oxyiodide reaction set, it is believed that the polyborate network is the main factor in determining the overall three-dimensional framework.[18] The rationale for this is the formation of an isotypic series when bromide and iodide are present. The only unique compound obtained was $Nd_4[B_{18}O_{25}(OH)_{13}Br_3]$. If the halide was responsible for any direction of the overall arrangement, it would be expected that a change in the structure would have been observed in going from the bromide to iodide series because the latter is much larger than the former. The same cannot be said for the products of this work. It appears that the halide has a much greater role in the formation of the overall structure. The two biggest indications of this are observed in the **NdBOBr** and **LnBOI** products.

In **NdBOBr**, we see for the first time terminal halides bound to the base sites of the metal centers. Because they are terminal, this removes a potential layer joining coordination sites, which limits the options for joining the layers together. Furthermore, this reduces the negative charge associated with the overall framework (i.e., Br^- vs BO_3^{3-}/BO_4^{5-}) because generally borate groups are found on the base sites. This likely induced the formation of a cationic framework. For the **LnBOI** series, the large capping and terminal iodine atom requires a "double" connection in order to provide the necessary space. Because the **LnBOI** compounds have only water on the base sites, the extra negative charge is obtained from the additional BO_3^{3-} unit in the double connection, allowing for an overall neutral framework.

It is interesting that, in both the oxyiodide and concentrated HI reaction sets, the resulting products result in an isotypic series for each respective reaction set.[18] While it has been demonstrated that the building units of borates, BO_3 triangles and BO_4 tetrahedra, can polymerize to form countless types of polyborate anions, which provide numerous bonding modes to coordinate the metal centers with a variety of geometric requirements,[1−4] it appears that, at high iodine concentrations, the large iodine atoms play a greater role in determining the optimal overall framework structure and can dictate the need for a "double" connection between the layers. The majority of trivalent lanthanide and actinide borates contain only BO_3 units between the layers and that holds true for these reaction sets.[15−18,22]

CONCLUSIONS

In this report, we found that the trivalent lanthanide products obtained from a boric acid flux with the addition of concentrated HBr or HI results in individual/discrete compounds for the former and an isostructural series of compounds for the latter. When compared to the analogous compounds obtained from our previous study starting with the tribromide/oxyiodide, the new bromide series has much more variability as far as the structure is concerned and the new iodide series result in another, yet different, isostructural set. This variability between these two sets of reactions (tribromide/oxyiodide versus concentrated HBr/HI) demonstrates just how sensitive the borate system is to experimental conditions. This sensitivity to experimental conditions can be used to provide a means for the synthesis of a variety of compounds.

It is our conclusion that, while the borate network helps to direct the unusual geometries observed, the counteranions play a role, because of size and/or coordination, in how the layers are tethered (single versus double connection) to yield the resulting three-dimensional structure. Moreover, the halides have the ability to be either terminal or bridging. It can now be said that bromide can reside exclusively on the base sites of the metal and the halogens should not be regarded as capping/apical ligands only.

ASSOCIATED CONTENT

Supporting Information

X-ray crystallographic data in CIF format and powder diffraction data. This material is available free of charge via the Internet at http://pubs.acs.org.

AUTHOR INFORMATION

Corresponding Author

*E-mail: talbrechtschmitt@gmail.com.

Notes

The authors declare no competing financial interest.

ACKNOWLEDGMENTS

We are grateful for support provided by the Chemical Sciences, Geosciences, and Biosciences Division, Office of Basic Energy Sciences, Office of Science, Heavy Elements Chemistry Program, U.S. Department of Energy, under Grant DE-FG02-09ER16026. Collaborative work with our German counterparts is supported via the Helmholtz Association (Grant VH-NG-815).

REFERENCES

(1) Burns, P. C.; Grice, J. D.; Hawthorne, F. C. *Can. Mineral.* **1995**, *33*, 1131.

(2) Grice, J. D.; Burns, P. C.; Hawthorne, F. C. *Can. Mineral.* **1999**, *37*, 731.

(3) Yuan, G.; Xue, D. *Acta Crystallogr.* **2007**, *B63*, 353.

(4) Krivovichev, S.; Burns, P. C.; Tananaev, I. G. *Structural Chemistry of Inorganic Actinide Compounds*; Elsevier: Dordrecht, The Netherlands, 2007.

(5) (a) Giesber, H.; Ballato, J.; Chumanov, G.; Kolis, J.; Dejneka, M. *J. Appl. Phys.* **2003**, *93*, 8987. (b) Giesber, H.; Ballato, J.; Pennington, W. T.; Kolis, J. W.; Dejneka, M. *Glass Technol.* **2003**, *44*, 42.

(6) Saubat, B.; Fouassier, C.; Hagenmuller, P.; Bourcet, J. C. *Mater. Res. Bull.* **1981**, *16*, 193–198.

(7) Machida, K.; Adachi, G.; Shiokawa, J. *J. Lumin.* **1979**, *21*, 101–110.

(8) Pei, Z. W.; Su, Q.; Zhang, J. Y. *J. Alloys Compd.* **1993**, *198*, 51−53.
(9) Chen, C. T. Development of New Nonlinear Optical Crystals in the Borate Series. *Laser Science and Technical International Handbook*; Harwood: New York, 1993; Vol. *15*.
(10) Snider, A. C. *Verification of the Definition of Generic Weep Brine and the Development of a Recipe for this Brine*; ERMS 527505; Sandia National Laboratories: Carlsbad, NM, 2003.
(11) *Compliance Recertification Application for the Waste Isolation Pilot Plant Appendix SOTERM 2009*; U.S. Department of Energy: Washington, DC, 2009.
(12) Borkowski, M.; Richmann, M.; Reed, D. T.; Xiong, Y. *Radiochim. Acta* **2010**, *98*, 577−582.
(13) Park, J.-H.; Chopra, O. K.; Natesan, K.; Shack, W. J.; Cullen, W. H., Jr. *Boric Acid Corrosion of Light Water Reactor Pressure Vessel Materials*; Argonne National Laboratory: Chicago, IL, 2005.
(14) Burns, P. C.; Ewing, R. C.; Navrotsky, A. *Science* **2012**, *335*, 1184−1188.
(15) Polinski, M. J.; Wang, S.; Alekseev, E. V.; Depmeier, W.; Albrecht-Schmitt, T. E. *Angew. Chem., Int. Ed.* **2011**, *50*, 8891−8894.
(16) Polinski, M. J.; Wang, S.; Alekseev, E. V.; Depmeier, W.; Liu, G.; Haire, R. G.; Albrecht-Schmitt, T. E. *Angew. Chem., Int. Ed.* **2012**, *51*, 1869−1872.
(17) Polinski, M. J.; Grant, D. J.; Wang, S.; Alekseev, E. V.; Cross, J. N.; Villa, E. M.; Depmeier, W.; Gagliardi, L.; Albrecht-Schmitt, T. E. *J. Am. Chem. Soc.* **2012**, *134*, 10682−10692.
(18) Polinski, M. J.; Wang, S.; Cross, J. N.; Alekseev, E. V.; Depmeier, W.; Albrecht-Schmitt, T. E. *Inorg. Chem.* **2012**, *51*, 7859−7866.
(19) SADABS 2001, Program for absorption correction using SMART CCD based on the method of R. H. Blessing: Sheldrick, G. M. *Acta Crystallogr.* **1995**, *A51*, 33.
(20) Sheldrick, G. M. *Acta Crystallogr.* **2008**, *A46*, 112−122.
(21) Ruiz-Martínez, A.; Alverz, S. *Chem.—Eur. J.* **2009**, *15*, 7470−7480.
(22) Wang, S.; Alekseev, E. V.; Depmeier, W.; Albrecht-Schmitt, T. E. *Inorg. Chem.* **2011**, *50*, 2079−2081.
(23) Li, L.; Jin, X.; Li, G.; Wang, Y.; Liao, F.; Tao, G.; Lin, J. *Chem. Mater.* **2003**, *15*, 2253−2260.
(24) Ruiz-Martínez, A.; Casanova, D.; Alverz, S. *Chem.—Eur. J.* **2008**, *14*, 1291−1303.
(25) Wang, S.; Alekseev, E. V.; Depmeier, W.; Albrecht-Schmitt, T. E. *Chem. Commun.* **2011**, *47*, 10874−10885.
(26) *Layered Double Hydroxides: Present and Future*; Rives, V., Ed.; Nova Science: New York, 2001.
(27) Wang, S.; Alekseev, E. V.; Diwu, J.; Casey, W. H.; Phillips, B. L.; Depmeier, W.; Albrecht-Schmitt, T. E. *Angew. Chem., Int. Ed.* **2010**, *49*, 1057−1060.
(28) Wang, S.; Ping, Y.; Purse, B. A.; Orta, M. J.; Diwu, J.; Casey, W. H.; Phillips, B. L.; Alekseev, E. A.; Depmeier, W.; Hobbs, D. T.; Albrecht-Schmitt, T. E. *Adv. Funct. Mater.* **2012**, *22*, 2241−2250.
(29) Polinski, M. J.; Wang, S.; Alekseev, E. V.; Cross, J. N.; Depmeier, W.; Albrecht-Schmitt, T. E. *Inorg. Chem.* **2012**, *51*, 11541−11548.